Investigation of rehomogenization in the framework of nodal cross section corrections

Gamarino, M.; Tomatis, D.; Dall'Osso, A.; Lathouwers, D.; Kloosterman, J. L.; Van Der Hagen, T. H.J.J.

Publication date
2016

Document Version
Final published version

Published in
Physics of Reactors 2016, PHYSOR 2016: Unifying Theory and Experiments in the 21st Century

Investigation of rehomogenization in the framework of nodal cross section corrections

Gamarino, Matteo; Tomatis, D.; Dall'Osso, A.; Lathouwers, Danny; Kloosterman, Jan-Leen; van der Hagen, Tim

Publication date
2016

Document Version
Final published version

Published in
Physics of Reactors 2016, PHYSOR 2016: Unifying Theory and Experiments in the 21st Century

Citation (APA)
Gamarino, M., Tomatis, D., Dall'Osso, A., Lathouwers, D., Kloosterman, J. L., & Van Der Hagen, T. H. J. J. (2016). Investigation of rehomogenization in the framework of nodal cross section corrections. In Physics of Reactors 2016, PHYSOR 2016: Unifying Theory and Experiments in the 21st Century (Vol. 6, pp. 3698-3707). American Nuclear Society.

Important note
To cite this publication, please use the final published version (if applicable).
Please check the document version above.

INVESTIGATION OF REHOMOGENIZATION IN THE FRAMEWORK OF NODAL CROSS SECTION CORRECTIONS

M. Gamarino [*1], D. Tomatis[2], A. Dall'Osso[2], D. Lathouwers[1], J.L. Kloosterman[1], and T.H.J.J. van der Hagen[1]

[1]Department of Nuclear Energy and Radiation Applications, Delft University of Technology, Mekelweg 15, 2629 JB Delft, The Netherlands
[2]AREVA NP, Tour AREVA, 92084 Paris La Défense Cedex, France

ABSTRACT

Few-group cross sections used in nodal calculations derive from standard energy collapsing and spatial homogenization performed during preliminary lattice transport calculations, that implicitly assume an infinite array of identical fuel-assemblies. The infinite-medium neutron flux used for cross section weighting does not account for environmental effects arising in case of heterogeneous configurations, which can lead to considerable leakages out of or into the assembly and thus invalidate the reflective boundary conditions used for the lattice simulation. Core-environment effects can also cause variations, with respect to the infinite-lattice calculation, in the reference cross section distribution used for few-group constant collapsing. These sources of inaccuracy prevent from reproducing with high fidelity the best estimate of the reaction rates and multiplication factor coming from the reference transport global solution. Rehomogenization techniques are therefore needed. The purpose of the present paper, which builds upon previous work done at AREVA in the area of rehomogenization, is to formalize a mathematical model that encompasses the different kinds of homogenization errors. In order to investigate the accuracy of the corresponding cross section corrections, numerical tests of an assembly-configuration sample are presented.

Key Words: **Nodal diffusion; Spatial and Spectral Rehomogenization; Cross section correction; Burn-up.**

1. INTRODUCTION

Current deterministic methodologies for nuclear reactor core analysis make wide use of nodal diffusion approaches [1]. Cross sections used in nodal codes for 3-D core simulations are generally obtained by energy collapsing and spatial homogenization from single-assembly calculations with reflective boundary conditions (also referred to as infinite-medium conditions in the following) [2]. Their preparation involves a set of reference cross sections in a very fine number of energy groups and a reference condensation flux determined by neutron transport in the most detailed geometry. If the assembly is far away from the reflector and surrounded by assemblies of the same type in a large medium compared to the neutron mean free path, this assumption is clearly acceptable. However, when the assembly is in its real environment (i.e., the reactor core), the neutron flux distribution can differ significantly from the one calculated in the infinite medium due to different boundary conditions. Common examples are mixed MOX/UO_2 fuel loading patterns, heterogeneous configurations with depletable strong local absorbers and controlled regions [3, 4]. Environmental conditions should be modeled with these layouts to reproduce more accurate nodal cross sections, still using the homogenization paradigm. Smith first

*Corresponding author: M.Gamarino@tudelft.nl

suggested an approach of cross section rehomogenization to correct the flux-induced homogenization error [5]. Recently, other rehomogenization techniques have been developed independently at AREVA NP addressing separately the error in space and in energy [6–8].
Other sources of inaccuracy can arise in nodal cross section preparation. Cross section models used in core calculations adopt generally only one depletion history in PWRs, thus fixing the evolution of the isotopic content in the assembly [9]. This issue is still present with simulations in BWRs, even if the corresponding models use more depletion evolutions for considering the coolant void history as additional state parameter [10]. Hence, depletion modules have to track important isotopes and perform a history correction to the nodal cross sections. Moreover, due to self-shielding and within-cell flux distribution the environmental effects can cause variations in the fine-group pin-by-pin microscopic cross section distribution at assembly borders and in the nuclide densities with respect to the base depletion in the infinite-medium lattice calculation. Therefore it is necessary to account also for a homogenization defect due to the change of the reference cross section set used for few-group constant collapsing in the real environment. Contrary to flux-induced defects reproduced by corrective terms, which are prepared with the standard parameterized tables, defects associated to the cross section distribution are usually treated online in the core calculation. This implementation was first proposed by Wagner et al. [11]. Since the correction is based on the burn-up reconstruction in each node, it is simply called burn-up cross section correction.
The aim of this paper is to propose a theoretical model classifying nodal cross section corrections and evaluate the relative benefits on the accuracy of nodal calculations for a test case. Our work is meant to formalize the spatial and spectral rehomogenization techniques developed at AREVA NP and the burnup-dependent correction in a comprehensive and consistent analytical framework, proving the complementarity of the corresponding adjustments. The model here presented is being benchmarked by numerical simulation of several heterogeneous assembly-configurations. In the present paper, the results of a nodal diffusion solver, recently developed in the context of a joint PhD project between AREVA NP and TU Delft, are compared to the reference values from neutron transport determined by the spectral code APOLLO2-A. Focus is given to the spatial and spectral effects of the environment.

2. A MATHEMATICAL MODEL FOR CROSS SECTION CORRECTIONS

A formal derivation of the environmental correction of the few-group nodal cross section $\Sigma^{(h)}_{g,env}$ for a given reaction is performed (superscript h here stands for "homogenized"). An analytical expression for the global homogenization defect $\delta\Sigma_g$ is derived by means of the environmental flux and cross section distributions Φ_{env} and Σ_{env}, provided in the fine multigroup formalism. The phase space is limited to space $\mathbf{r}$ and energy E for use with nodal diffusion codes. Both environmental quantities are defined in each node as sum of the reference distribution in infinite-medium conditions, used at cross section preparation by the lattice code, and of a smooth function δ. Hence the environmental flux and cross section become:

$$\Phi_{env} = \Phi_{\infty} + \delta\Phi, \tag{1a}$$

$$\Sigma_{env} = \Sigma_{\infty} + \delta\Sigma. \tag{1b}$$

In our model the term $\delta\Sigma$ appearing in Equation (1b) is only due to depleting with the environmental flux instead of the infinite-medium one (effects associated to self-shielding and within-cell flux distribution are not taken into account). The cross section condensed in the g-th coarse group and homogenized in the real environmental conditions in the node of volume $V^{(n)}$ is defined as:

$$\Sigma_{g,env}^{(h,n)} = \frac{\int_{V^{(n)}} d\mathbf{r} \int_{E_{g+1}}^{E_g} dE\ \Sigma_{env}(\mathbf{r},E)\Phi_{env}(\mathbf{r},E)}{\int_{V^{(n)}} d\mathbf{r} \int_{E_{g+1}}^{E_g} dE\ \Phi_{env}(\mathbf{r},E)}. \quad (2)$$

As a convention, in the proposed model the environmental and infinite-medium fluxes are scaled to have the same node-average value $\Phi_{avg,g}^{(n)}$ inside each energy group, that is:

$$\int_{V^{(n)}} d\mathbf{r} \int_{E_{g+1}}^{E_g} dE\ \Phi_{\infty,g}(\mathbf{r},E) = \int_{V^{(n)}} d\mathbf{r} \int_{E_{g+1}}^{E_g} dE\ \Phi_{env,g}(\mathbf{r},E) = \Phi_{avg,g}^{(n)} V^{(n)} = \mathcal{F}_g^{(n)}. \quad (3)$$

The best-estimate of $\Phi_{avg,g}^{(n)}$ is one of the outputs of the nodal calculation. If we replace the flux distribution along the whole energy axis (Φ_{env}) by the one within group g ($\Phi_{env,g}$) in Equation (2), using Equations (1)-(3) the following expression for $\Sigma_{g,env}^{(h,n)}$ can be achieved:

$$\Sigma_{g,env}^{(h,n)} = \Sigma_{g,\infty}^{(h,n)} + \delta\Sigma_g^{(r,n)} + \delta\Sigma_g^{(xs,n)}, \quad (4)$$

with:

- $\Sigma_{g,\infty}^{(h,n)}$ as the nodal cross section interpolated from libraries at the current values of the state parameters in the node n:

$$\Sigma_{g,\infty}^{(h,n)} = \frac{1}{\mathcal{F}_g^{(n)}} \int_{V^{(n)}} d\mathbf{r} \int_{E_{g+1}}^{E_g} dE\ \Sigma_\infty(\mathbf{r},E)\Phi_{\infty,g}(\mathbf{r},E); \quad (5)$$

- $\delta\Sigma_g^{(r,n)}$ as the homogenization defect due to the flux variation:

$$\delta\Sigma_g^{(r,n)} = \frac{1}{\mathcal{F}_g^{(n)}} \int_{V^{(n)}} d\mathbf{r} \int_{E_{g+1}}^{E_g} dE\ \Sigma_\infty(\mathbf{r},E)\delta\Phi_g(\mathbf{r},E); \quad (6)$$

- $\delta\Sigma_g^{(xs,n)}$ as the homogenization error due to variations in the fine cross section distribution related to the depletion in the real environment:

$$\delta\Sigma_g^{(xs,n)} = \frac{1}{\mathcal{F}_g^{(n)}} \int_{V^{(n)}} d\mathbf{r} \int_{E_{g+1}}^{E_g} dE\ \delta\Sigma(\mathbf{r},E)\Phi_{env,g}(\mathbf{r},E). \quad (7)$$

The leading term from Equation (5) corresponds to the coarse-group cross section homogenized in the infinite-medium conditions. This is the output of standard single-assembly transport calculations performed by spectral codes.

The term detailed in Equation (6) is reproduced in the present work by the rehomogenization methods developed at AREVA NP [6–8]. These approaches consist of estimating the difference between the environmental flux distribution and the infinite-lattice one by means of a limited set of known modal components in the domain of space and energy. Rigorously, spatial and spectral effects of the environment are tightly coupled [3]. A full rehomogenization model where the space and energy dimensions are considered simultaneously can be put forward by defining the aforementioned flux variation for group g and spatial domain $V^{(n)}$ as follows:

$$\delta\Phi_g(\mathbf{r},E) = \sum_i \sum_j \gamma_{ij,g} \cdot P_{i,g}(\mathbf{r}) \cdot Q_{j,g}(E) + \epsilon_{rehom,g} \quad (8)$$

being $P_{i,g}(\mathbf{r})$ and $Q_{j,g}(E)$ basis functions ranging from analytical functions to physically justified modes. The rehomogenization error $\epsilon_{rehom,g}$ accounts for the fact that the trial set might not form a

complete base of the phase space under study. As first attempt to simplify the correction term of Equation (6), the flux variation $\delta\Phi_g$ can be further elaborated to separate the spectral and spatial effects of the environment, thus easing the computation and using the current rehomogenization strategies [6–8]. The corresponding derivation, detailed in Appendix A, results in the following expression for $\delta\Sigma_g^{(r,n)}$:

$$\delta\Sigma_g^{(r,n)} \approx \delta\Sigma_g^{(spat,n)} + \delta\Sigma_g^{(spectr,n)} + \delta\Sigma_g^{(cross,n)}. \tag{9}$$

The cross-correction $\delta\Sigma_g^{(cross,n)}$ appearing in Equation (9) derives from mixed space-energy terms. It is not accounted for in the current implementation of the rehomogenization model.
As for the term of Equation (7), the application of the mean value theorem for integration in energy yields:

$$\frac{1}{\mathcal{F}_g^{(n)}} \int_{V^{(n)}} d\mathbf{r} \int_{E_{g+1}}^{E_g} dE\, \delta\Sigma(\mathbf{r},E)\Phi_{env,g}(\mathbf{r},E) = \frac{1}{\mathcal{F}_g^{(n)}} \int_{V^{(n)}} d\mathbf{r}\, \delta\Sigma_g(\mathbf{r})\Phi_{env,g}(\mathbf{r}). \tag{10}$$

Corrections due to variations of the fine cross section distribution in the real environment can thus be considered as averaged in each coarse group of the core simulation. The calculation of this adjustment is approached by imposing some intra-assembly spatial dependence on the nodal cross sections, modeling burn-up induced heterogeneities. We include in this term the cross section correction of Wagner, Koebke and Winter [11].

3. APPLICATION TO A UO_2 COLORSET WITH PYREX

The test case here presented is a 2-D colorset consisting of four 17×17 PWR fuel assemblies of fresh UO_2 with two different compositions: the former with 1.8 % enrichment, the latter with 3.1 % enrichment and 16 rods containing burnable absorber (Pyrex). The assembly set is depicted in Figure 1.

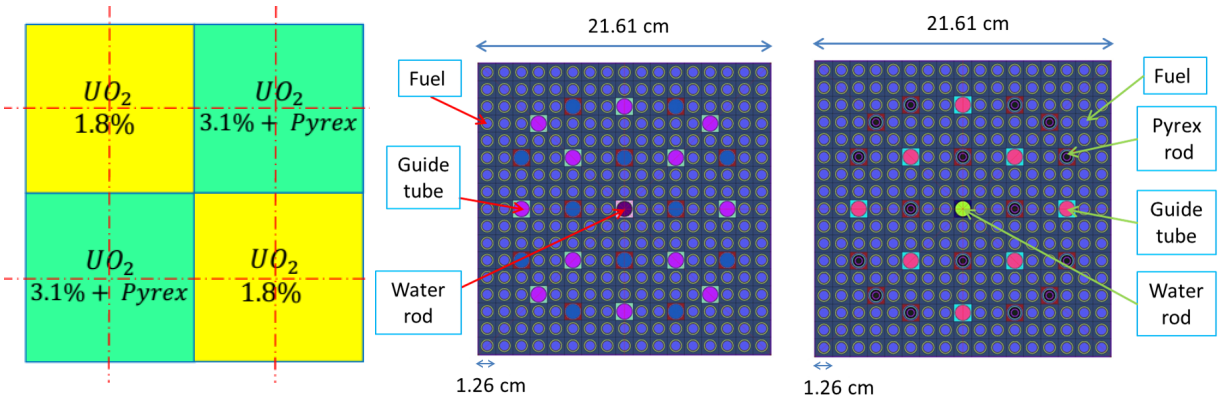

Figure 1: Assembly-set under study (a) and layout of UO_2 fuel assemblies with 1.8 % enrichment (b) and 3.1 % enrichment and Pyrex (c). Symmetry axis along which reflective boundary conditions are set are shown in (a). A nodalization of 2×2 nodes per assembly is chosen.

The nodal diffusion solver adopted in this work is based on a traditional non-linear CMFD-NEM coupling [1], and uses standard parameterized tables computed in APOLLO2-A. The values of the main state parameters correspond to hot full power conditions; the concentration of B_{10} is set to 700 ppm.

Fresh initial core conditions are considered: as the burn-up is uniformly zero within the nodes, the depletion correction term of Equation (7) is neglected. In order to investigate the effects of spatial and spectral corrections, four different nodal simulations are performed: with infinite-medium homogenization parameters (*a*), with spatial rehomogenization of cross sections and discontinuity factors (*b*), with spectral rehomogenization of cross sections (*c*) and with spatial and spectral rehomogenization applied sequentially (*d*). It is remarked that, at the current state of development, spatial rehomogenization does not correct scattering cross sections and the diffusion coefficient. When solving the spectral rehomogenization problem, as a temporary implementation the fine-group energy shape of the transverse leakage is taken as input data from the reference solution, which comes from a fine heterogeneous transport calculation made in APOLLO2-A for the whole colorset. In the final implementation this shape will be computed using nodal information.
The flux shape variation between the real environment and the infinite-medium conditions estimated by rehomogenization is plotted in Figure 2 for the space domain and in Figure 3 for energy. A very good reconstruction is found for the spatial flux variation, which is more important in the thermal range (especially for the heterogeneous assembly). The computed spectrum variation exhibits some inaccuracy in the high energy peak region of the fast range (around 10 MeV) and at the interface between the two coarse groups (i.e., around 0.625 eV), where the change has higher magnitude.

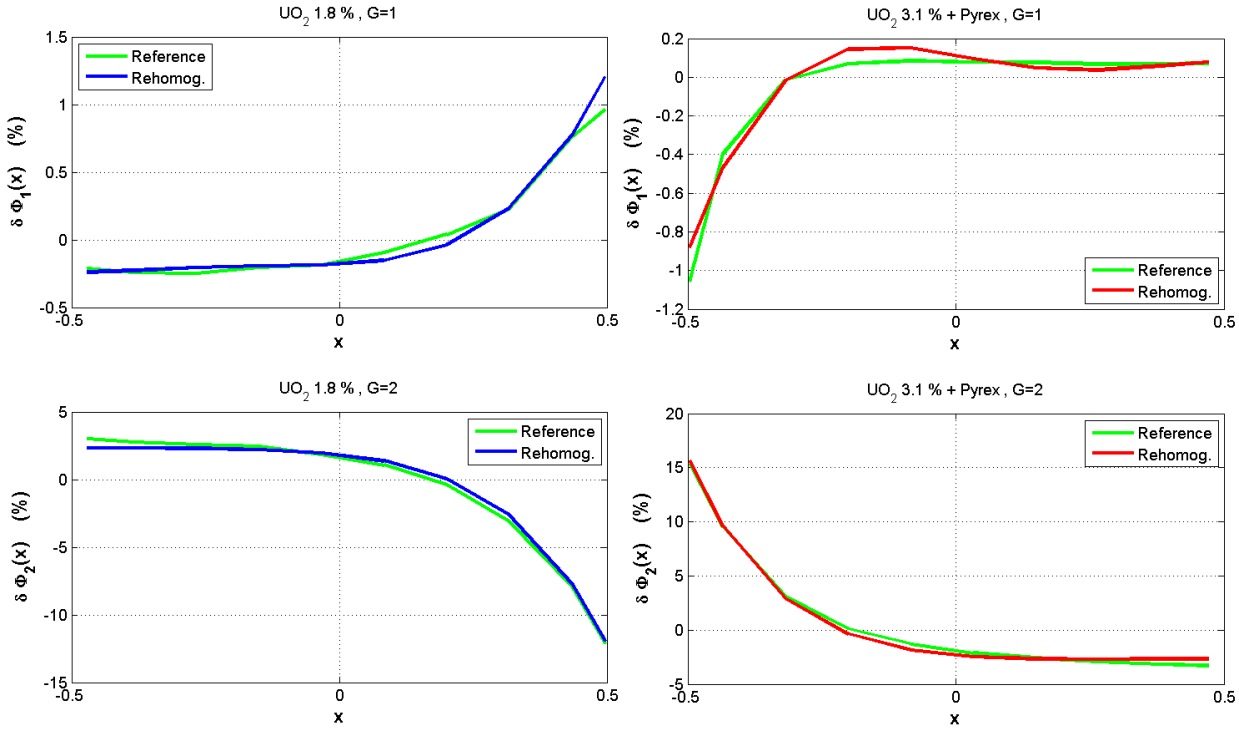

Figure 2: Variation in the transverse-integrated spatial flux distribution computed from the reference calculation and estimated by spatial rehomogenization. Non-dimensional coordinates are used ($x = 0$ corresponds to the center of the node). As for the heterogeneous assembly, since the fast and thermal flux variations are respectively positive and negative in the center of the bundle (where Pyrex rods are mostly located and neutron absorption is thus higher), it turns that $\delta\Sigma_{a,1}^{spat} > 0$ and $\delta\Sigma_{a,2}^{spat} < 0$.

The results in terms of multiplication factor and nodal power distribution for the four calculations are shown in Table I. A significant improvement is found with calculations (*b*) and (*d*). The spatial and

spectral effects of the environment go in the same direction, which leads to a small over-correction of k_{eff} and to a reversal of the nodal power error sign when the two rehomogenization techniques are applied sequentially. In order to have a better insight into the accuracy of the method, the errors on the main nodal cross sections are shown in Table II. Apart from thermal absorption in the assembly containing burnable poison, stand-alone spatial and spectral rehomogenizations lead to a general improvement of cross sections. Excellent results are found when the two corrections are combined.

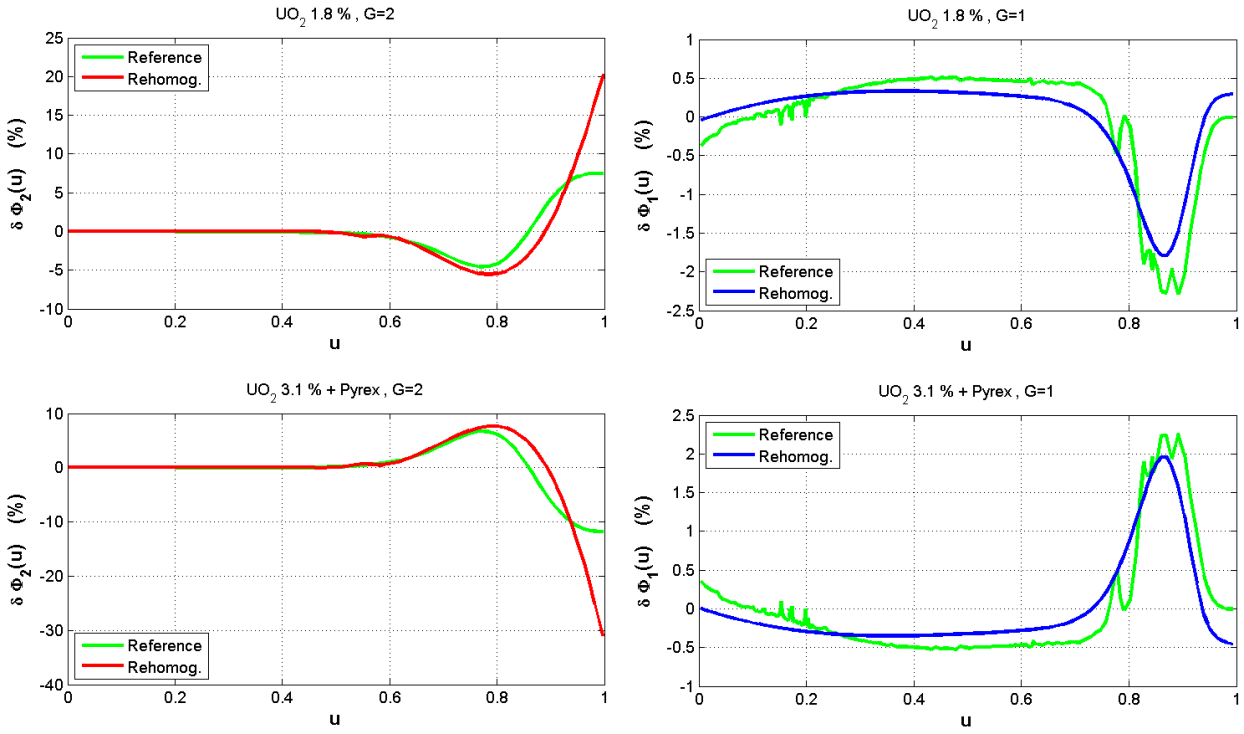

Figure 3: Spectrum variation per unit lethargy computed from the reference calculation and estimated by spectral rehomogenization. Lethargy is defined separately in the coarse groups according to [7]. As for the assembly with Pyrex, within G=1 the computed spectrum variation is negative in the epithermal range, whereas within G=2 it is positive above the thermal equilibrium region; hence, due to fission and absorption cross section energy-dependence inside the coarse groups, the relative corrections are negative for G=1 and positive for G=2. Opposite considerations hold for the homogeneous assembly.

Table I: Comparison of multiplication factor (k_{eff}) and nodal power distribution (P_{avg}). Normalized reference values of P_{avg} are 0.934 for the assembly without Pyrex and 1.066 for the assembly with Pyrex.

			UO_2 1.8 %	UO_2 3.1 % + Pyrex
Simulation	k_{eff}	Δk_{eff} [pcm]	Error on P_{avg} (%)	Error on P_{avg} (%)
Reference	1.08462	-		
Standard (a)	1.08215	-247	1.171	-1.025
Spatial rehom. (b)	1.08442	-20	0.326	-0.286
Spectral rehom. (c)	1.08249	-213	0.679	-0.594
Spatial + spectral rehom. (d)	1.08478	+16	-0.430	0.376

Table II: Errors (%) on nodal cross sections for the assembly with 1.8 % enrichment (a) and the one with 3.1 % enrichment and Pyrex rods (b). Significant improvement or deterioration (in terms of the absolute value of the error) is highlighted in blue and red, respectively.

UO_2 1.8 %	$\Sigma_{a,1}$	$\Sigma_{a,2}$	$\nu\Sigma_{f,1}$	$\nu\Sigma_{f,2}$	$\Sigma_{t,1}$	$\Sigma_{t,2}$
Reference [cm^{-1}]	0.008538	0.061314	0.004827	0.081858	0.530798	1.27959
Simulation			Error %			
Standard (*a*)	-0.198	0.732	0.379	0.823	-0.218	0.254
Spatial rehom. (*b*)	-0.191	0.653	0.387	0.705	-0.217	0.250
Spectral rehom. (*c*)	0.182	-0.044	0.421	0.014	-0.040	-0.156
Spatial + spectral rehom. (*d*)	-0.069	-0.097	-0.078	-0.077	-0.056	-0.146

(a)

UO_2 3.1 % + Pyrex	$\Sigma_{a,1}$	$\Sigma_{a,2}$	$\nu\Sigma_{f,1}$	$\nu\Sigma_{f,2}$	$\Sigma_{t,1}$	$\Sigma_{t,2}$
Reference [cm^{-1}]	0.009945	0.096917	0.006570	0.132247	0.518613	1.26863
Simulation			Error %			
Standard (*a*)	0.194	-0.476	-0.233	-1.103	0.219	-0.471
Spatial rehom. (*b*)	0.204	-0.903	-0.236	-0.990	0.219	-0.504
Spectral rehom. (*c*)	-0.223	0.592	-0.402	0.061	0.034	0.127
Spatial + spectral rehom. (*d*)	-0.065	0.098	0.047	0.110	0.053	0.062

(b)

Errors on scattering cross sections are reported in Table III.

Table III: Errors (%) on scattering cross sections.

	UO_2 1.8 %				UO_2 3.1 % + Pyrex			
	$\Sigma_{s,1\to1}$	$\Sigma_{s,1\to2}$	$\Sigma_{s,2\to1}$	$\Sigma_{s,2\to2}$	$\Sigma_{s,1\to1}$	$\Sigma_{s,1\to2}$	$\Sigma_{s,2\to1}$	$\Sigma_{s,2\to2}$
Reference [cm^{-1}]	0.504911	0.017387	0.001282	1.21699	0.493194	0.015513	0.001748	1.16997
Simulation			Error %				Error %	
Calc. (*a*) and (*b*)	-0.235	0.274	-5.18	0.236	0.236	-0.307	6.02	-0.481
Spectral rehom. (*c*)	-0.058	0.392	9.84	-0.172	0.055	-0.478	-10.4	0.105
Spatial + spectral rehom. (*d*)	-0.061	0.090	9.11	-0.158	0.058	-0.125	-9.16	0.073

Cases in which spectral rehomogenization is applied experience in general a remarkable improvement. A significant over-correction trend is found for out-scattering in the thermal group, which, however, is of negligible amount.

Potential vanishing of favorable error cancellation is found to be a weakness of rehomogenization. Indeed even though the method enables a considerable reduction of errors on nodal cross sections, in some cases an equally noteworthy enhancement in integral parameters is not observed. From the analysis of Tables I and II, for instance, despite Σ-related inaccuracies become negligible for calculation (*d*), the lowest errors on nodal power characterize simulation (*b*). As spatial rehomogenization does not adjust scattering cross sections yet, adding a correction reproducing only the spectral effect might

overshadow error compensation in case the spatial one goes in the opposite direction. Calculation (*d*) was thus repeated without changing out- and self-scattering cross sections. It was found that inaccuracies on k_{eff}, as well as on absorption and production cross sections, stay similar in magnitude, whereas the error on nodal power drops to -0.167 % for the assembly without Pyrex and +0.146 % for the assembly with Pyrex. This might be a consequence of the aforementioned error offset due to using infinite-medium scattering cross sections.
Error compensation is expected to play a relevant role in depletion calculations. In assemblies where nodal power is overestimated, the fuel initially burns more and loses reactivity more rapidly, which leads to a reduction of the power itself (inversely in bundles where power is underestimated). In simulations performed with infinite-medium cross sections at low burn-up values, the power is overvalued in the less reactive assembly (UO_2 1.8 %) and undervalued in the more reactive one (UO_2 3.1 % with burnable absorber), as found for fresh fuel in Table I. Therefore, the error on the multiplication factor (which is initially negative) is reduced for increasing values of burn-up. As the decrease of the error on nodal power due to cross section corrections goes in the opposite direction with respect to this "self-healing" effect, the benefits of rehomogenization might be partly concealed.

4. CONCLUSIONS

A theoretical model classifying nodal cross section corrections has been presented. Spatial and spectral rehomogenization have been applied to a test case representative of the environmental effects observable in a reactor core, and proved to improve significantly the results with respect to the standard calculation using infinite-medium homogenization parameters.
A global framework for cross section corrections is deemed to be a milestone in the context of nodal simulations, for which so far the work reported in literature has only considered the different kinds of environmental adjustments individually. Work is currently being performed to enhance the accuracy of rehomogenization by modeling the effects of spatial and spectral heterogeneity to a greater extent. Further developments to be pursued include the incorporation of spatial and spectral corrections in a simultaneous approach and the investigation of configurations including burn-up, where depletion defects and self-healing effects become relevant. An analysis of the interplay among these corrections applied all together will give useful insight into the effect of the environment on the global solution of the neutron diffusion problem in the reactor core, and enable to improve the performance of current nodal core simulations.

REFERENCES

[1] R. Lawrence. "Progress in nodal methods for the solution of the neutron diffusion and transport equations." *Progress in Nuclear Energy*, **17(3)**: pp. 271–301 (1986).

[2] K. S. Smith. "Assembly homogenization techniques for Light Water Reactor analysis." *Progress in Nuclear Energy*, **17(3)**: pp. 303–335 (1986).

[3] S. P. Palmtag. *Advanced nodal methods for MOX fuel analysis*. Ph.D. thesis, Massachusetts Institute of Technology (1997).

[4] K. T. Clarno and M. L. Adams. "Capturing the effects of unlike neighbors in single-assembly calculations." *Nuclear science and engineering*, **149(2)**: pp. 182–196 (2005).

[5] K. Smith. "Practical and efficient iterative method for LWR fuel assembly homogenization." *Transactions of the American Nuclear Society*, **71** (1994).

[6] A. Dall'Osso. "A spatial rehomogenization method in nodal calculations." *Annals of Nuclear Energy*, **33(10)**: pp. 869–877 (2006).

[7] A. Dall'Osso, D. Tomatis, and Y. Du. "Improving cross sections via spectral rehomogenization." In: *Proc. of Int. Conf. PHYSOR*, (pp. 9–14) (2010).

[8] A. Dall'Osso. "Spatial rehomogenization of cross sections and discontinuity factors for nodal calculations." In: *Proc. of Int. Conf. PHYSOR* (2014).

[9] S. Sánchez-Cervera *et al.* "Optimization of multidimensional cross-section tables for few-group core calculations." *Annals of Nuclear Energy*, **69**: pp. 226–237 (2014).

[10] V. Marotte *et al.* "Industrial application of APOLLO2 to Boiling Water Reactors." In: *Proc. Int. Conf. Advances in Nuclear Analysis and Simulation (PHYSOR 2006)*, (pp. 10–14) (2006).

[11] M. Wagner, K. Koebke, and H.-J. Winter. "A non-linear extension of the nodal expansion method." In: *Proc. of Int. Conf. in Advances in Mathematical Methods for the Solution of Engineering Problems, Munich, Germany*, volume 2 (1981).

APPENDIX A. DERIVATION OF THE FLUX HOMOGENIZATION DEFECT

This Appendix reports a consistent derivation of the rehomogenization techniques developed at AREVA from the formulation proposed in Section 2.
The following factorization for the infinite-medium flux distribution is introduced:

$$\Phi_{\infty,g}(\mathbf{r},E) = \Phi_{\infty,g}(\mathbf{r}) \cdot \varphi_{\infty,g}(\mathbf{r},E), \tag{11}$$

where $\Phi_{\infty,g}(\mathbf{r})$ is the flux integrated in the coarse energy group g, while $\varphi_{\infty,g}(\mathbf{r},E)$ is a normalized spectrum having unitary average value within g. This factorization is always possible, and both factors are known by the spectral lattice transport calculation. An analogous factorization is considered for the environmental flux distribution:

$$\Phi_{env,g}(\mathbf{r},E) = \Phi_{env,g}(\mathbf{r}) \cdot \varphi_{env,g}(\mathbf{r},E). \tag{12}$$

It is recalled that $\Phi_{env,g}(\mathbf{r},E)$ and $\Phi_{\infty,g}(\mathbf{r},E)$ are scaled to have the same average value $\Phi^{(n)}_{avg,g}$ within the node n (Equation (3)). According to Equation (6) and to the flux factorization of Equations (11) and (12), we write the $\delta\Phi_g$-related homogenization defect as:

$$\delta\Sigma_g^{(r,n)} = \frac{1}{\mathcal{F}_g^{(n)}} \int_{V^{(n)}} d\mathbf{r} \int_{E_{g+1}}^{E_g} dE\, \Sigma_\infty(\mathbf{r},E)\Phi_{env,g}(\mathbf{r})\varphi_{env,g}(\mathbf{r},E) - \frac{1}{\mathcal{F}_g^{(n)}} \int_{V^{(n)}} d\mathbf{r} \int_{E_{g+1}}^{E_g} dE\, \Sigma_\infty(\mathbf{r},E)\Phi_{\infty,g}(\mathbf{r})\varphi_{\infty,g}(\mathbf{r},E) \tag{13}$$

Consistently with the procedure used so far (Equation (1a)), the normalized spectrum in environmental conditions can be defined as the sum of the infinite-medium one and of a local variation term $\delta\varphi_g(\mathbf{r},E)$, having zero average value within the energy group g:

$$\varphi_{env,g}(\mathbf{r},E) = \varphi_{\infty,g}(\mathbf{r},E) + \delta\varphi_g(\mathbf{r},E) \tag{14}$$

Introducing Equation (14) and the spatial flux variation $\delta\Phi_g(\mathbf{r}) = \Phi_{env,g}(\mathbf{r}) - \Phi_{\infty,g}(\mathbf{r})$ (with zero volume-average within the fuel-assembly) into Equation (13), after some algebraic manipulation it

reduces as follows:

$$\delta\Sigma_g^{(r,n)} = \frac{1}{\mathcal{F}_g^{(n)}} \int_{V^{(n)}} d\mathbf{r} \int_{E_{g+1}}^{E_g} dE\, \Sigma_\infty(\mathbf{r},E)\delta\Phi_g(\mathbf{r})\varphi_{\infty,g}(\mathbf{r},E) + \frac{1}{\mathcal{F}_g^{(n)}} \int_{V^{(n)}} d\mathbf{r} \int_{E_{g+1}}^{E_g} dE\, \Sigma_\infty(\mathbf{r},E)\Phi_{env,g}(\mathbf{r})\delta\varphi_g(\mathbf{r},E). \quad (15)$$

The infinite-medium energy-collapsed spatial cross section distribution $\Sigma_{\infty,g}(\mathbf{r})$ can be defined as:

$$\Sigma_{\infty,g}(\mathbf{r}) = \frac{\int_{E_{g+1}}^{E_g} dE\, \Sigma_\infty(\mathbf{r},E)\varphi_{\infty,g}(\mathbf{r},E)}{\int_{E_{g+1}}^{E_g} dE\, \varphi_{\infty,g}(\mathbf{r},E)} \quad (16)$$

Hence, using Equation (16) the first term on the right-hand side of Equation (15) becomes:

$$\frac{1}{\Phi_{avg,g}^{(n)} V^{(n)}} \int_{V^{(n)}} d\mathbf{r}\, \Sigma_{\infty,g}(\mathbf{r})\delta\Phi_g(\mathbf{r}) = \delta\Sigma_g^{(spat,n)}, \quad (17)$$

that is the cross section correction defined in the framework of the spatial rehomogenization technique described in [6] and [8].
By means of Equation (1a), the second integral on the right-hand side of Equation (15) is rewritten as follows:

$$\int_{V^{(n)}} d\mathbf{r} \int_{E_{g+1}}^{E_g} dE\, \Sigma_\infty(\mathbf{r},E)\Phi_{env,g}(\mathbf{r})\delta\varphi_g(\mathbf{r},E) = \int_{V^{(n)}} d\mathbf{r} \int_{E_{g+1}}^{E_g} dE\, \Sigma_\infty(\mathbf{r},E)\Phi_{\infty,g}(\mathbf{r})\delta\varphi_g(\mathbf{r},E) + \int_{V^{(n)}} d\mathbf{r} \int_{E_{g+1}}^{E_g} dE\, \Sigma_\infty(\mathbf{r},E)\delta\Phi_g(\mathbf{r})\delta\varphi_g(\mathbf{r},E). \quad (18)$$

A cross-term correction can be identified:

$$\delta\Sigma_g^{cross,n} = \frac{1}{\mathcal{F}_g^{(n)}} \int_{V^{(n)}} d\mathbf{r} \int_{E_{g+1}}^{E_g} dE\, \Sigma_\infty(\mathbf{r},E)\delta\Phi_g(\mathbf{r})\delta\varphi_g(\mathbf{r},E). \quad (19)$$

At this point, an equivalent spectrum variation $\delta\varphi_{equiv,g}(E)$ is introduced:

$$\delta\varphi_{equiv,g}(E) = \frac{1}{\mathcal{F}_g^{(n)}} \frac{\int_{V^{(n)}} d\mathbf{r}\, \Sigma_\infty(\mathbf{r},E)\Phi_{\infty,g}(\mathbf{r})\delta\varphi_g(\mathbf{r},E)}{\int_{V^{(n)}} d\mathbf{r}\, \Sigma_\infty(\mathbf{r},E)\Phi_{\infty,g}(\mathbf{r})}. \quad (20)$$

After defining the infinite-medium spatially-homogenized cross section energy distribution $\Sigma_{hom,g}(E)$ as:

$$\Sigma_{hom,g}(E) = \frac{\int_{V^{(n)}} d\mathbf{r}\, \Sigma_\infty(\mathbf{r},E)\Phi_{\infty,g}(\mathbf{r})}{\int_{V^{(n)}} d\mathbf{r}\, \Phi_{\infty,g}(\mathbf{r})}, \quad (21)$$

the last addend of Equation (18) becomes:

$$\frac{1}{\Phi_{avg,g}^{(n)} V^{(n)}} \int_{E_{g+1}}^{E_g} dE\, \Sigma_{hom,g}(E)\delta\varphi_{equiv,g}(E) \approx \delta\Sigma_g^{(spectr,n)}. \quad (22)$$

This term can be assimilated to the cross section correction defined in the spectral rehomogenization method presented in [7]. The symbol $\approx$ is used instead of full equality because the term $\delta\varphi_{equiv,g}(E)$ is here an equivalent average spectrum change (i.e., a weighted average of $\delta\varphi_g(\mathbf{r},E)$), whereas in [7] it is the change in the spectrum relative to the average cross section.
Using Equations (17), (19) and (22), the definition of Equation (9) for the homogenization flux defect is achieved.